World Academy of Science, Engineering and Technology
International Journal of Electronics and Communication Engineering
Vol:7, No:8, 2013

A Novel Low-Profile Coupled-Fed Printed Twelve-Band Mobile Phone Antenna with Slotted Ground Plane for LTE/GSM/UMTS/WIMAX/WLAN Operations

Omar A. Saraereh, M. A. Smadi, A. K. S. Al-Bayati, Jasim A. Ghaeb, Qais H. Alsafasfeh

***Abstract*—**A low profile planar antenna for twelve-band operation in the mobile phone is presented. The proposed antenna radiating elements occupy an area equals 17×50 mm^2 are mounted on the compact no-ground portion of the system circuit board to achieve a simple low profile structure. In order to overcome the shortcoming of narrow bandwidth for conventional planar printed antenna, a novel bandwidth enhancement approach for multiband handset antennas is proposed here. The technique used in this study shows that by using a coupled-fed mechanism and a slotted ground structure, a multiband operation with wideband characteristic can be achieved. The influences of the modifications introduced into the ground plane improved significantly the bandwidths of the designed antenna. The slotted ground plane structure with the coupled-fed elements contributes their lowest, middle and higher-order resonant modes to form four operating modes. The generated modes are able to cover LTE 700/2300/2500, GSM 850/900/1800/1900, UMTS, WiMAX 3500, WLAN 2400/5200/5800 operations. Parametric studies via simulation are provided and discussed. Proposed antenna's gain, efficiency and radiation pattern characteristics over the desired operating bands are obtained and discussed. The reasonable results observed can meet the requirements of practical mobile phones.

***Keywords*—**Antenna, handset, LTE, Mobile, Multiband, Slotted ground, specific absorption rate (SAR).

I. Introduction

NOW days wireless communication systems are growing dramatically and more applications have been integrated in mobile devices, which means that mobile phone antennas need to be able to operate at a wide range of different applications. These applications evolve from analog to digital 2G (GSM), then to high data rate cellular wireless communications such as 3G (WCDMA), and further to packet optimized 3.5G (HSPA) and 4G (LTE and LTE advanced) systems [1].Therefore, antenna designs should be capable of covering the following frequency bands: LTE700 (698-787 MHz), GSM850 (824-896 MHz), GSM900 (880-960 MHz), GSM1800 (1710-1880 MHz), GSM1900 (1850-1990 MHz), UMTS (1920-2170 MHz), LTE2300 (2305-2400 MHz), WLAN2400 (2400-2484 MHz), LTE2500 (2500-2690 MHz), WiMAX (3400-3600 MHz), WLAN5200 (5150-5350) MHz and WLAN5800 (5725-5825) MHz. As a result, it is observable that more and more frequency bands are in service and increasing demands for antenna designs that have multisystem in multiband, compact size, low profile, wide bandwidth and built-in structures are necessary [2]. Moreover, there is a severe need for meeting the SAR standards and requirements due to health issues and standard regulations. In the literature, many antenna designs in the form of PIFAs (planar inverted-F antennas) [3], planar printed monopoles [4], fractals [5], arrays of multiple radiating elements [6] and folded structures [7] were able to cover several frequency bands of the aforementioned standards. In [8], [9] seven frequency bands have been achieved using coupled-fed planar printed monopole with bottom radiators. Eight operating bands have been obtained in [10], [11]. A coupled loop of 7 mm height with two branch lines has been used in [10] and planar printed monopole with shorted parasitic and bottom radiator proposed in [11]. However, in [12] an eleven band antenna design presented in the form of folded coupled-fed shorted monopole with poor performance at the lower LTE700 band (efficiency less than 45% at approximately 6 dB return loss).

It can be noted from published papers that the advantages of the planar printed monopole support the attributes of compact size and multi frequency operations [4], [8], [10]-[12]. The only drawback in this form of antennas is the narrow bandwidth, especially at the lower bands such as LTE700/GSM850/GSM900 which require outsized electrical length. In order to overcome the shortcoming of narrow bandwidth for conventional planar printed antenna, a novel bandwidth enhancement approach for internal multiband handset antennas is proposed in this article. Wideband characteristics can be accomplished using wideband radiating element [13] or arrays of multiple radiating elements [6], which are able to afford wideband responses at the expense of large electrical size, interference and necessity for additional front-end matching circuits. Another approach consists in using folded monopole structures [14] resulting in complex 3-D configurations that may be complicated to optimize and fabricate. Other techniques based on parasitic elements, solar

Omar A. Saraereh, M. A. Smadi, A. K. S. Al-Bayati, andJasim A. Ghaebare with the Electrical Engineering Department, The Hashemite University, Zarqa, 13115 Jordan (phone: +962 (0) 5 3903333 ext.4456; fax:+962 (0) 5 3826348; e-mail: eloas2@hu.edu.jo).

Qais H. Alsafasfeh is now with the Department of Electrical Engineerings, Tafila Technical University, Tafila, 66110 Jordan (e-mail: qshashim@ yahoo.com).

cells [15], tapered structure and active lumped circuit elements (capacitors, inductors and switches) has been reported [16]. Only a limited bandwidth is obtained using these techniques to cover several standard mobile phone applications.

The bandwidth enhancement approaches mentioned earlier focus on making modifications on the antenna's radiating element. However, there are also other bandwidth enhancement methods concentrating on making modifications on the system ground plane of a mobile handset [17]. The technique used in this study shows that by using a planar printed monopole antenna which combines a coupled-fed radiating element with a meandered shorted coupling strip and a slotted ground plane, a multiband operation with wideband characteristic can be achieved. These appropriate modifications, introduced within the system ground plane, can effectively adjust the electrical lengths of the ground plane to the optimal lengths required by the low and high bands. The ground structure in the presented design may act as a radiating element due to the alteration in the current distribution and consequently influences the antenna radiation performance. The different driven strips, meandered strips and slotted ground plane structure contribute their lowest, middle and higher-order resonant modes to form four wide operating bandwidths (return loss > 6 dB).

In this paper, we propose a novel multiband internal antenna with the size of $17 \times 50 \times 0.8\text{mm}^3$. This antenna is capable of generating four wide operating bands that effectively cover twelve standard operations in mobile phone LTE/GSM/UMTS/WiMAX/WLAN. The antenna's four wide operating bands are achieved and controlled by tuning the dimensions of the introduced slots and notches in the ground plane structure, the gaps between the feeding and shorting strips in addition to the meandered shapes presented in the design. Parametric studies via simulation are carried out and antenna's typical performance for frequencies over the desired operating bands has been obtained and discussed. The proposed antenna is suitable to be directly printed on the system circuit board of the mobile phone, making it easy to fabricate at low cost and attractive for slim mobile phone applications.

II. Antenna Structure and Design Process

Fig. 1 (a) illustrates a top view of the proposed planar antenna configuration and dimensions. The antenna radiating elements developed within the top area of printed circuit board (PCB) to occupy an area of $17 \times 50\text{mm}^2$. The main ground is printed on a 0.8mm thick FR-4 substrate (relative permittivity 4.4 and loss tangent is 0.02) of total size $50 \times 120\text{mm}^2$ according to recent smart phone applications. The dimensions of the PCB and the ground size considered here are practical for general smart phones or personal digital assistant (PDA) phones that are available in the market. The system ground plane of size $50 \times 105.4\text{mm}^2$ is printed on the back side of the circuit board, leaving a no-ground portion of a size $14.6 \times 50\text{mm}^2$ at the top region of the PCB as depicted in Fig. 1 (b). The no-ground area of the proposed antenna with coupled feeding structure is introduced. A 50 Ω coaxial feed line is employed to excite the antenna and a shorting pin (via) is functioned to connect between the shorted coupling strip and the ground region of the PCB. In order to broaden the bandwidth of the presented antenna, different slots and notches has been introduced into the system ground plane as shown in Fig. 1 (b). More detailed operating mechanism of the coupled-fed antenna and the slotted ground plane will be illustrated and discussed later. The plastic housing cover is also considered for the real mobile terminal situation. The plastic material utilized is ABS polymer (relative permittivity is 3.3 and loss tangent 0.02). The housing cover has dimensions of $54 \times 130\text{mm}^2$ with 1mm thickness. It has also a 3 mm gap between the antenna and the inner housing cover. The selected dimensions allow the system circuit board to be at the center of the plastic housing.

The proposed antenna can provide twelve-band LTE/GSM/UMTS/WiMAX/WLAN operating bands with return loss better than 6 dB. The first operating band (694-107 MHz) is able to cover the LTE 700 and GSM 850/900 operations, while the second operating band (1707-2737 MHz) allows GSM 1800/1900, UMTS, LTE 2300/2500 and WLAN 2400 operations. The third operating band (3363-3614 MHz) covers WiMAX 3500 and finally the highest operating band (5096-5819 MHz) covers WLAN 5200/5800.

In this scheme, the metal pattern of the antenna mainly comprises three parts: a longer coupling strip, a shorter feeding strip and slotted ground plane structure at the lower edge of the no-ground portion as depicted in Fig. 2. In one hand, the coupling strip includes two U-shapes, pointed to as U_{c1}, U_{c2} in Fig. 2, with meandered arms m_1 and m_2 added for each shape respectively. A coupling stub of 0.3 mm width is added as well to U_{c2} for tuning purposes. On the other hand, the feeding strip formed by a slotted L-shape and a U-shape named as L_f andU_f in Fig.2. The slotted ground plane structure consists of three different length slots (s_1, s_2, and s_3) with uniform width 1 mm and two notches (n_1, n_2) as shown in Fig. 1 (b). The main objective of using the aforementioned sensible combination between the coupled feeding structure and the slotted ground plane is to create multiple resonances and improve the bandwidth at the required resonant modes observably [17], [18].

The feeding strip (L_f,U_f) alone can function as resourceful λ/4 radiator to generate a resonant mode around 2600 MHz. Coupling strip U_{c2} correlated with the feeding strip through a small coupling gap (g_1) and the resulted couple structure can achieve the impedance matching to provide a wide band (1950-3350 MHz) operation. They can also generate a resonance path at 1100 MHz which can be investigated to provide resonance mode at the lower bands LTE700/GSM850/GSM900. Strip U_{c1} contributes to the lower band operation (1000-1220 MHz) and enhances the middle band operation to cover (1750-3350 MHz). A coupling stub (0.3 mm wide) is added to U_{c2} to couple with U_f throughcoupling gape g_4 and generate a resonance mode at 900 MHz to afford a lower band operation (810-1000 MHz).Last but not least, two meandered branches (m_1, m_2) have been carefully added to strip (Uc_1, U_{c2}) to produce

resonance modes at 820 MHz (780-872 MHz), 2350MHz (1900-3100 MHz) and 4770 MHz (4650-4880 MHz).The proposed branches (m_1, m_2) are meandered to guarantee a compact antenna structure. The coupling effect between adjacent meandered elements makes the effective electrical length less than the physical length, which is fundamentally reason that the strip length of branch is larger than required λ/4.

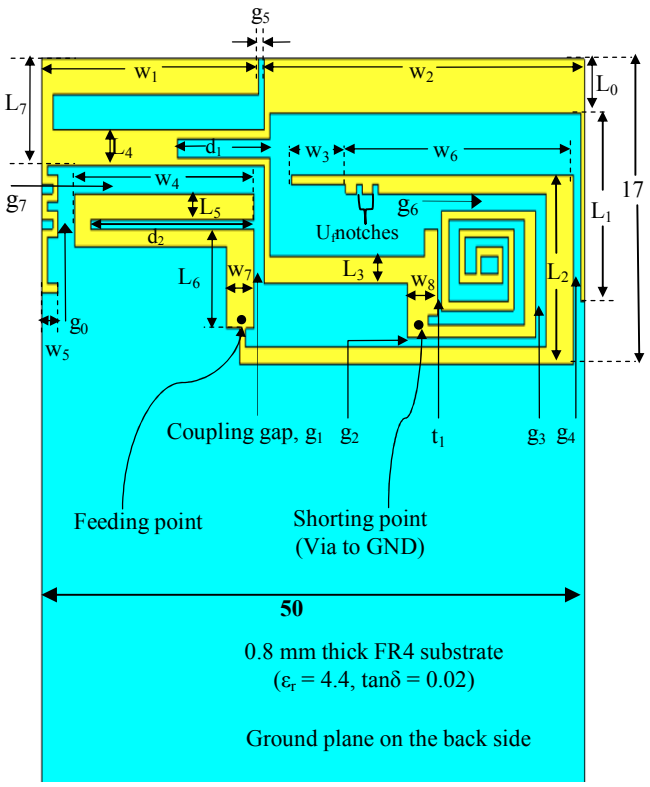

Fig. 1 (a) Proposed antenna configuration (front view) and detailed dimensions

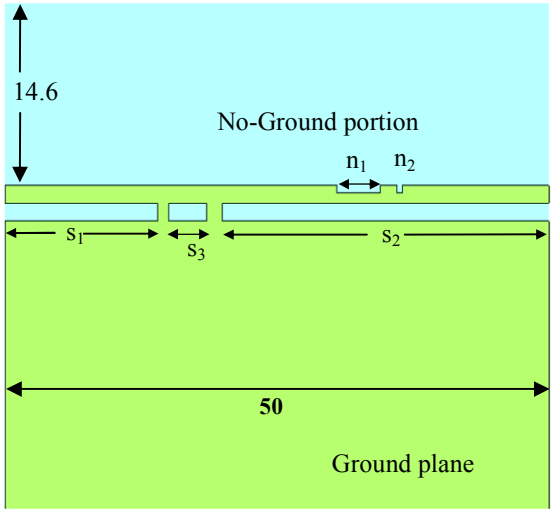

Fig. 1 (b) Proposed antenna slotted ground plane (bottom view)

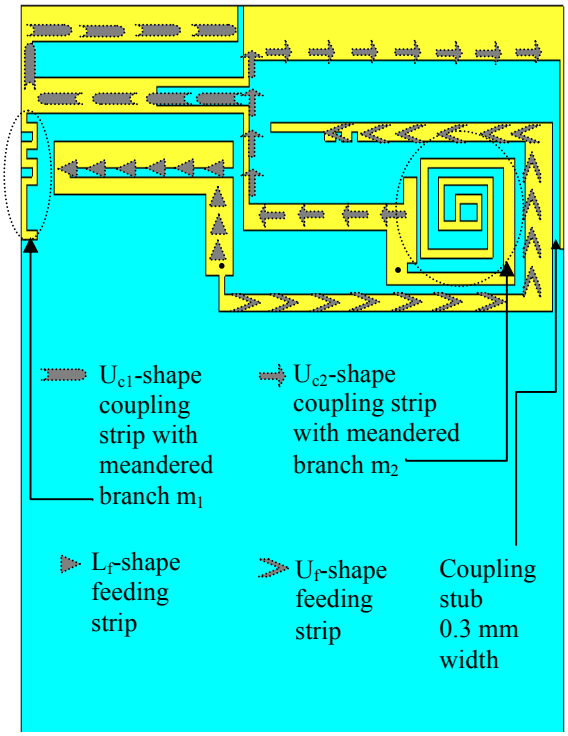

Fig. 2 The metal pattern of the presented antenna

A slot (d_1) has been created in the coupling strip U_{c1} to push the higher band at 4770 MHz to resonate at 5490 MHz to provide 480 MHz bandwidth operation. Another slot (d_2) is introduced to the feeding strip L_f as well to generate a resonance path at 3500 MHz and shift the lower band to resonate at 770 MHz with narrower bandwidth.

Finally, to enhance and tune the bandwidths of the achieved operating modes for the proposed conventional planar printed antenna, a slotted ground plane structure is used. The modified ground plane can help to achieve good impedance matching for frequencies over lower, middle and higher bands. A rigorous analysis has been carried out in order to establish the dimensions and position of slots (s_1, s_2, and s_3) and the two notches (n_1, n_2) in the ground plane as depicted in Fig. 1 (b). The main objective of the proposed modifications is to change the current distribution in the ground plane in order to achieve better excitation in the ground plane mode because it produces a longer electrical path for the ground plane surface currents. Slot (s_1) has been designed to improve the impedance bandwidth in the high frequency region resonating at 3500 MHz to form two adjacent resonances at 3420 MHz and 3552 MHz. It acts as a parasitic element which is coupled to the printed planar monopole. Parametric studies showed that the introduced slot should be positioned close to the proposed antenna configuration to guarantee good coupling with L_f, U_{c1} strips and achieve an optimum length of approximately quarter wavelength. Slot (s_2) is designed to be longer than s_1 and the best position for this slot is obtained when it is located in series with s_1 as shown Fig. 1 (b). The reason behind choosing this position is due to the fact that it is the location where the ground plane presents high current values and its current can

be easily modified. The slot with an optimum width couples with L_f, U_{c1} strips and the coupling stub to achieve an effective electrical length reaches 0.2 λ at 740 MHz, 0.27 λ at 1051MHz, 0.47λ at 1780 MHz and greater than half wavelength for the upper bands at 3500 MHz and 5500MHz. By means of introducing slot (s_2) in the ground plane, the bandwidth has significantly enhanced in the lower, middle and upper operating bands. A third shorter slot (s_3) has been inserted between s_1 and s_2 into the ground plane with two notches etched very close to the shorting pin via to shift the lower band to resonate at 720 MHz and cover the desired lower band (695-1068 MHz).

Furthermore, the impedance matching over the different frequency bands can also be controlled by adjusting the coupling gaps (g_0, g_1… g_6) between the feeding strip and the coupling strip. Other parameters and dimensions such as: w_3, w_5 and U_f strip notches have contributed efficiently to the antenna performance. The detailed effects are investigated and the geometric parameters of the antenna have been optimized through parametric studies as will be discussed in the coming sections. The optimization design has been carried out with the help of plentiful simulations using the electromagnetic computer-aided software CST Microwave Studio™. The optimized values for the geometric parameters are listed in Table I. In the rest of the article, all geometric parameters take for granted the values in this table unless they are given in particular. Fig. 3 shows the simulated results for return loss of the optimized planar printed monopole antenna. It can be noted that the simulated bandwidth (for return loss > 6 dB) has four operating wide bands around 880 MHz, 2220 MHz, 3480 MHz and 5457 MHz. With proper structure and dimensions, the proposed design can be simply printed on a thin PCB. Hence, the presented antenna not only illustrates simple configuration but also has a compact size, allowing it to be fabricated at low cost for practical mobile applications.

TABLE I
OPTIMIZED VALUES (mm) FOR THE GEOMETRIC PARAMETERS OF THE PROPOSEDANTENNA

Parameter	Value	Parameter	Value	Parameter	Value
L_0	3	w_1	20	g_0	1.5
L_1	13.5	w_2	29.5	g_1	1
L_2	7	w_3	5	g_2	0.5
L_3	1.5	w_4	16.5	g_3	1
L_4	2	w_5	1.5	g_4	0.7
L_5	1.5	w_6	21	g_5	0.5
L_6	5.5	w_7	2.5	g_6	1
L_7	6	w_8	2.8	g_7	1.5
t_1	0.3	s_1	14	n_1	4
d_1	8.5	s_2	30	n_2	0.5
d_2	15	s_3	3.5	$U_f$notches	0.5×0.5

III. PARAMETRIC STUDIES

To study the presented antenna behavior and characteristic performances, including the presence of the coupled-fed mechanism and the novel slotted ground plane structure, Fig. 4 shows a comparison of the simulated return losses of the optimized proposed antenna and the primary antenna designs (Des I: feeding strip L_f/ U_f only; Des II: coupling strip Uc_1/ U_{c2}, feeding strip Lf/U_f and coupling stub without slotted GND). It can be clearly seen that with use of the feeding strip only (Des I), there are no resonant modes at the lower band of 698-960 MHz and the higher bands of 3400-3600 MHz / 5150-5825 MHz. Moreover, for the case Des II (without slotted GND) the coupled-fed mechanism has generated multi-resonance at 900/1200/2200/30720 MHz. The results show that the desired bands are not covered completely, especially for LTE700/GSM1800 which they form a real challenge for antenna designers. The coupled-fed structure can be represented by two equivalent circuits electromagnetically coupled with each other as illustrated in [19].

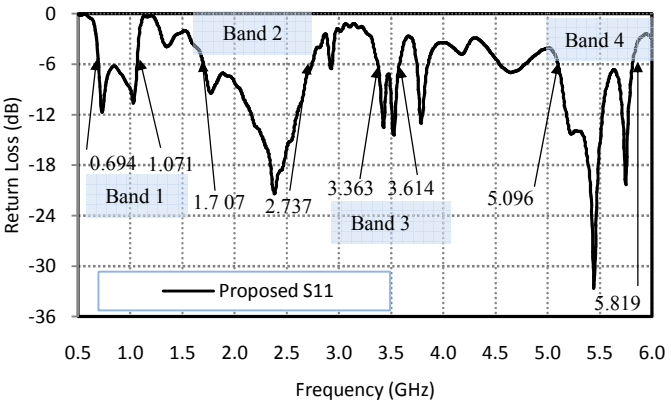

Fig. 3 Simulated results for return loss of the proposed antenna

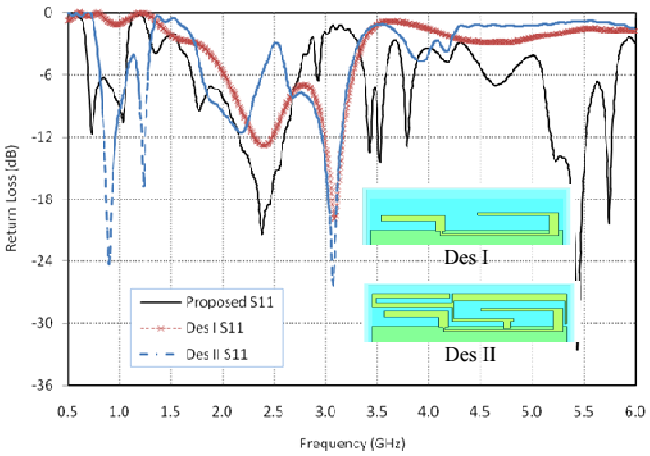

Fig. 4 Simulated return losses of the proposed antenna, the antennaprimarydesign with feeding strip only (Des I) and the corresponding coupled-fed structure without slotted GND (Des II)

In order to increase the coupling effect and the antenna's electrical length, Des II has been enlarged within the same allocated size by adding a meandered braches, slots, and notches to the feeding and coupling strips to produce Des III (without slotted GND). Fig. 5 shows a comparison of the simulated return losses of the proposed antenna and Des III. The comparison shows that Des III has four fundamental

frequency bands which require bandwidth enhancement and tuning to cover the desired standard operating bands. As a consequence, with the presence of the introduced slotted ground plane structure in the proposed antenna design there is a significant improvement can be distinguished in Fig. 5. The bandwidth is enhanced observably for band 2, band 3 and band 4, and it is clear that the desired resonant length of band1 in the lower modes is adjusted and improved to achieve a twelve-band LTE/GSM/UMTS/WiMAX/WLAN operation in the practical mobile phone applications.

Various vital parameters, of those listed in Table I, such as the coupling gap (g_5), ground plane slot (s_2), coupling stub length (L_1), continuity of the left meandered branch (w_5) and U_{c1} slot (d_1) are thoroughly investigated, so that their effects on impedance bandwidth can be determined. Through numerous CST simulations we found that the coupling gaps between the feeding and coupling strips at different locations have a considerable effect on the mutual coupling. Fig. 6 shows the effect of the coupling gap parameter g_5 on the impedance matching when the gap varies from 1 – 2.2mm. As the horizontal distance between the feeding strip and coupling strip in this location increases, the mutual coupling is degraded and the impedance matching around 5500 MHz (band4) lost completely and around 1850 MHz (band2) the return loss increased slightly. Thus, by selecting the proper value for g_5, the return loss can be improved as shown in Fig. 6 for the optimum value in the proposed antenna. The coupling gaps (g_0… g_7) between the feeding and coupling strips in the proposed antenna have been investigated as well to find their optimum values given in Table I.

Effects of varying the width (horizontal distance) of slot s_2 in the system ground plane are studied in Fig. 7. Results for width s_2 varied from 15 to 30 mm are presented. Band 2 at 2500 MHz and band 4 at 5500 MHz are seen to be affected significantly by width s_2. Band 1 has been slightly affected by this parameter, where it is clear that the lower mode is shifted up to lose approximately 24 MHz of the LTE700 bandwidth. Band 3 is stable under the variations in parameter s_2. By selecting a proper width s_2 (s_2 = 30 mm in the proposed design), good impedance matching over the desired bands can be achieved. Other parameters, such as s_1 and n_2, in the ground plane structure have been studied during this design and showed that they have a strong contribution to the impedance bandwidth of the proposed antenna, especially for the lower band which excites LTE700/GSM850/GSM900.

The simulated effect of varying the length of the coupling stub (L_1) in the proposed antenna is presented in Fig. 8. Here, it is obvious that the length L_1 is strongly responsible for the matching in band 1, band 3, band4 and increasing the bandwidth for band 2. It is observed that a decrease in L_1 will lead to a mismatch in band 1, band 3 and band 4. Nevertheless, the decrease in L_1 will improve the bandwidth significantly in band 2. Strong effects on the impedance matching of the frequencies over band 1, band 2, band 3 and band 4 are noted when the width of parameter w_5 is varied from the optimum value 1.5mm to a horizontal width 9mm as shown in Fig. 9. The impedance matching over band 3 is very poor around 3500 MHz. However, the impedance matching at band 1 and band 4 is degraded since the resonant mode of each band has been split to two different resonant modes with narrow bandwidths. Moreover, band 2 has lost approximately 50% of its bandwidth under this variation in w_5 width. Fig. 10 shows the simulated return losses relative to changes in the width of slot d_1. It can be noted that by reducing the width of d_1 from 8.5mm to 7.5mm the lower edge of band 1 shifted from 696 to 710 MHz, which resulting in a narrow bandwidth incapable of covering LTE700. Band 3 has largely affected by reducing d_1 width and the resonant mode covering the WiMAX band has been split to two narrow bands. In band 2 and 4 the bandwidth remained nearly constant. On the other hand, by increasing the width d_1 from 8.5mm to 10.5mm the results show that there is a strong impedance mismatch in band 1 band 4. Band 2 and band 3 have been slightly affected by this increment in d_1. Width d_1 is set at 8.5mm in the proposed antenna so as to cover the required operations.

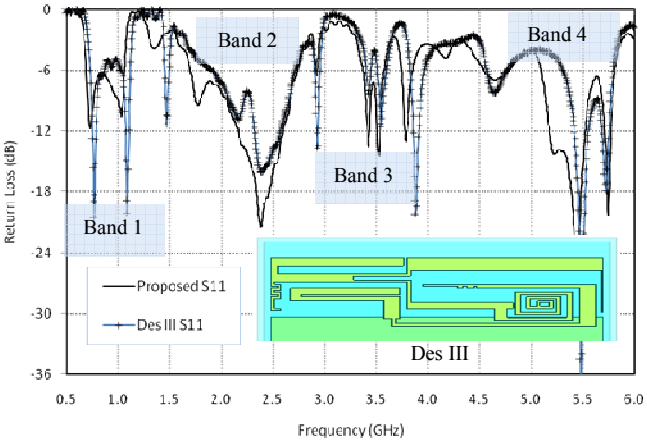

Fig. 5 Simulated return losses of proposed antenna and Des III (without slotted GND)

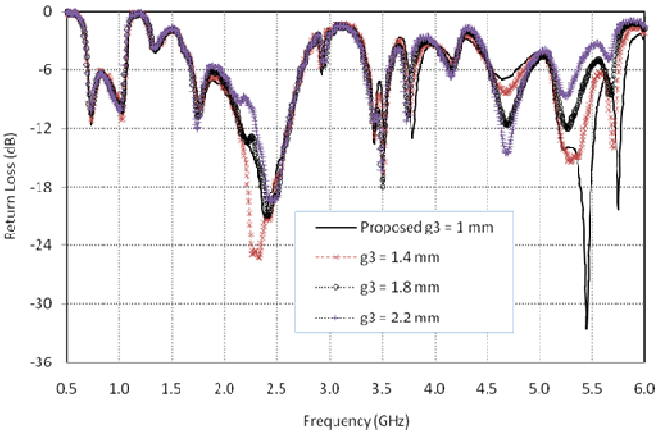

Fig. 6 Effect of the coupling gap g_3 on the return loss of proposed antenna, where g_3 has been changed from 1 mm to 2.2 mm

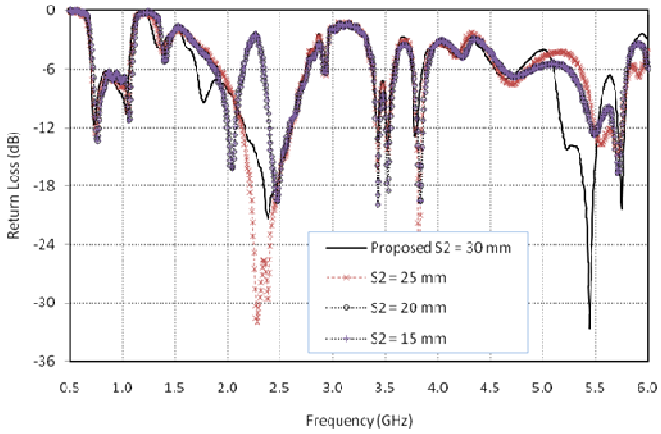

Fig. 7 Effect of the ground plane slot s_2 on the return loss of proposed antenna, where s_2 has been changed from 15 mm to 30 mm

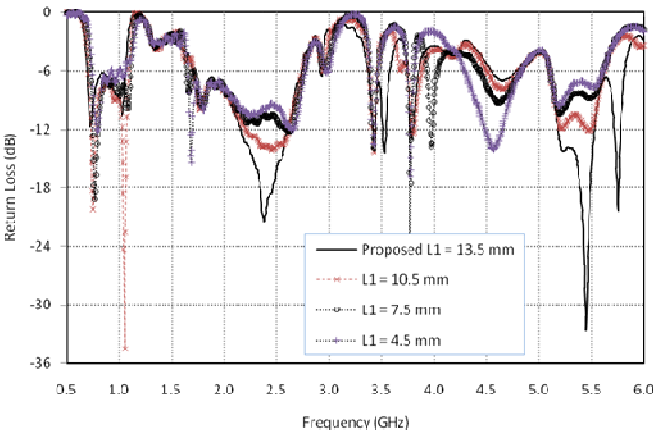

Fig. 8 Simulated return losses of proposed antenna when tuning the coupling stub length L_1 from 4.5mm to 13.5mm

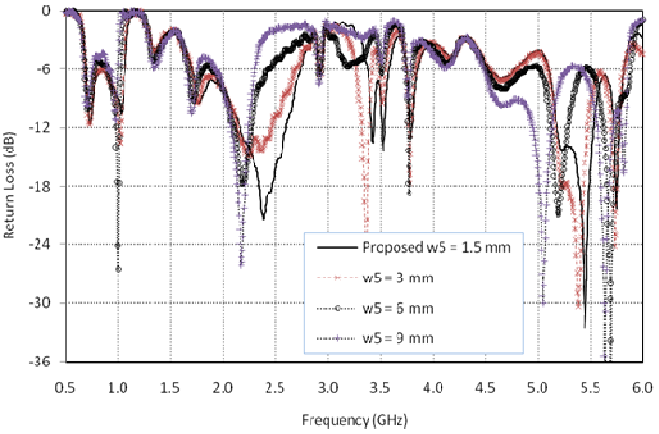

Fig. 9 Simulated return losses of proposed antenna when tuning parameter w_5 width from 1.5mm to 9mm

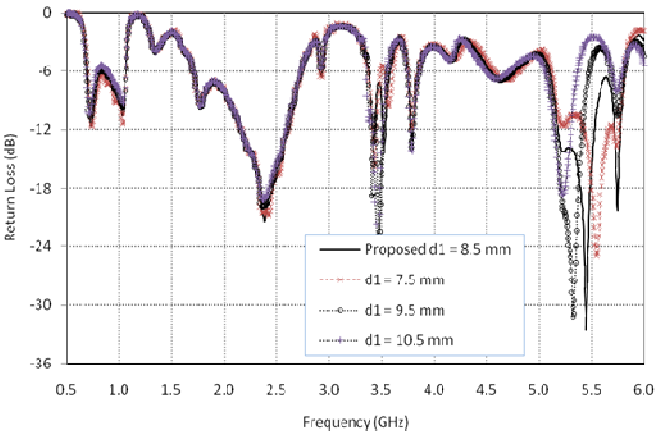

Fig. 10 Simulated return losses of proposed antenna when tuning parameter d_1 width from 7.5mm to 10.5mm

The effects of the ground plane size are also studied, where the simulated results show that the length of the system ground plane affects the performance of the antenna. The length of the ground plane has a great impact on the lower band. When the length reduced, the performance over band 1 highly degrades. However, good performance over the required operating bands is achieved at an optimum value 120 mm for the ground plane length. The width of the ground plane has little effect on the proposed antenna performance. The ground plane effects may also make supportive to the bandwidth of the lower mode LTE700/GSM850/GSM900. Fig. 11 shows the surface current distributions simulated on the antenna's top radiator and ground plane at 730, 920, 1900, 2350, 3500 and 5630 MHz. Fig. 11 (a) shows the surface current distributions at 730 MHz, where it can be seen relatively strong current distributions across the coupling strip, feeding strip and the slotted ground plane. At 920 MHz it is clear that the main contribution is for the feeding strip, part of the coupling strip and slightly the system ground plane as shown in Fig. 11 (b). However, at 1900 MHz the main contribution is for the feeding strip only with very minor contribution for the coupling strip and small effect for the ground plane as depicted in Fig. 11 (c). At 2350 MHz it is obvious from Fig. 11 (d) that the whole antenna configuration (feeding strip, coupling strip and slotted ground plane) makes an effective radiating system to cover band 2 (1703 -2742 MHz). The surface currents at 3500 MHz are given in Fig. 11 (d) and it is clear that they are mainly contributed by the feeding strip, coupling strip and the slots proposed in the antenna ground plane. Finally, at 5630 MHz the surface current distribution are strongly effective due to the feeding strip and slightly due to the coupling strip with very minor effect for the ground plane as shown in Fig. 11(e). It can be concluded from studying the surface current distributions that the system slotted ground plane structure is highly effective in enhancing the presented antenna performance in band 1 and band 2 which cover the standard operations LTE700/GSM850/GSM900/GSM 1800/1900/UMTS/LTE 230 0/2500/WLAN 2400.

IV. Results and Discussion

In order to verify the performance of the proposed planar printed monopole antenna, the design has been simulated using Ansoft HFSS software [20]. Fig. 12 show a comparison between the simulated return losses of the proposed antenna using CST Microwave Studio and Ansoft HFSS. It can be

clearly seen that both simulation methods provide extremely comparable results in all bands and good agreement for the four resonance modes of interest is achieved. The results show that the obtained frequency bands resonate at 730 MHz (bandwidth 368 MHz; 43%) , 2380 MHz (bandwidth 1040 MHz; 47%), 3420 MHz (bandwidth 220 MHz; 8%) and 5450 MHz (bandwidth 719 MHz; 14%) respectively, covering twelve communication bands (LTE 700, GSM 850/900, GSM 1800/1900, UMTS, LTE 2300/2500, WLAN 2400, WiMAX 3500 and WLAN 5200/5800) with return loss better than 6 dB. As international criterion, the 6 dB return loss (3:1 Voltage Standing Wave Ratio (VSWR)) definition is generally accepted for the internal mobile phone antenna operations.

The simulated antenna average gain and radiation efficiency for frequencies over the twelve operating bands are plotted in Fig. 13. The gain levels are stable through the operating bands and vary between 1.6 dB and 5.4 dB. The simulated radiation efficiency across the selected frequencies is better than 80%. Obviously, the higher bands (2, 3 and 4) have better performance compared to the lower band (band1) which covers LTE700/GSM850/GSM900. This drop in the lower mode behavior can be justified by the effects of the overlapped current cancellation between the coupled-fed structure and the slotted ground plane structure. The good radiation characteristics obtained over the antenna's four operating bands indicate that the proposed antenna is an acceptable solution for practical mobile applications.

Fig. 14 shows the simulated three-dimensional (3D) total power radiation patterns for the proposed antenna. Four radiation patterns can be seen from four different views (front, back, top and bottom). For lower frequency at 840 MHz in the first band and 2350 MHz in the second band the radiation patterns are close to those of a half-wave length dipole antenna and omnidirectional radiation with several nulls can be seen. This behavior indicates that the excited resonant modes in the second band are related to the higher-order modes of the conventional dipole antenna. At 3500 MHz in the third band and 5630 MHz in the fourth band, more variations with dips and nulls in the radiation pattern are seen. This is mainly because the system ground of the presented antenna is also an effective radiator and has dimensions much larger than the wavelengths of the operating frequencies, which strongly affects the radiation patterns.

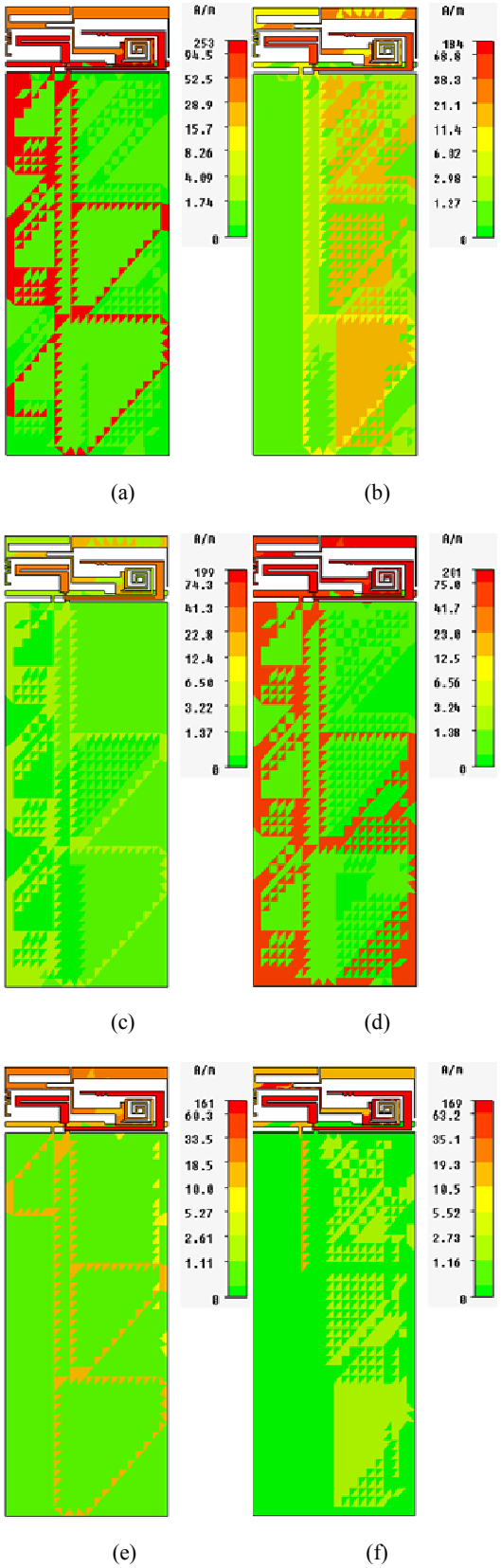

Fig. 11 Surface current distribution simulated on the proposed antenna top radiator and ground plane at (a) 730 MHz, (b) 920 MHz, (c) 1900 MHz, (d) 2350 MHz, (e) 3500 MHz and (f) 5630 MHz

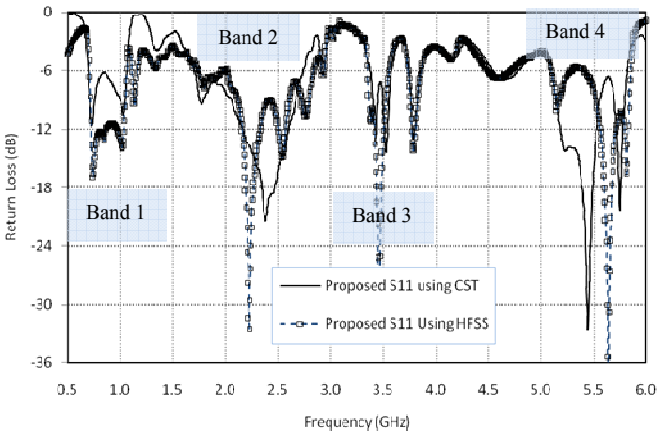

Fig. 12 Simulated return losses of proposed antenna using CST and HFSS simulation packages

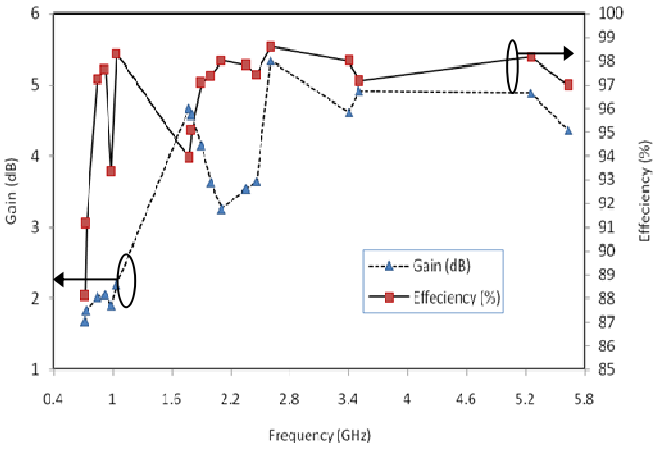

Fig. 13 Simulated average gains and simulated radiation efficiencies of the proposed antenna at different four resonance bands

A final test for the proposed handset antenna is to evaluate it in the presence of a human head in terms of a unit referred to as SAR. It is very important to investigate and analyze the interaction between human head and the presented handset antenna with the new proposed slotted ground plan. SAR value is strongly dependent on the ground plane geometry and the antenna position [21]. The SAR value used in the assessment of mobile phones measures the amount ofEM energy absorbed by human tissue. The SAR is expressed mathematically by measuring the electric field in the simulated human tissue in close vicinity to the device under test as given in (1) [22]:

$$SAR = \sigma \mid E \mid^2 / \rho = J^2 / \rho \, \sigma \, [\mathrm{W/Kg}] \qquad (1)$$

E: rms value of the electric strength in the tissue [V/m]; J: Current density [A/m]; σ: Conductivity of body tissue [S/m]; ρ: Density of body tissues [Kg/m^3]

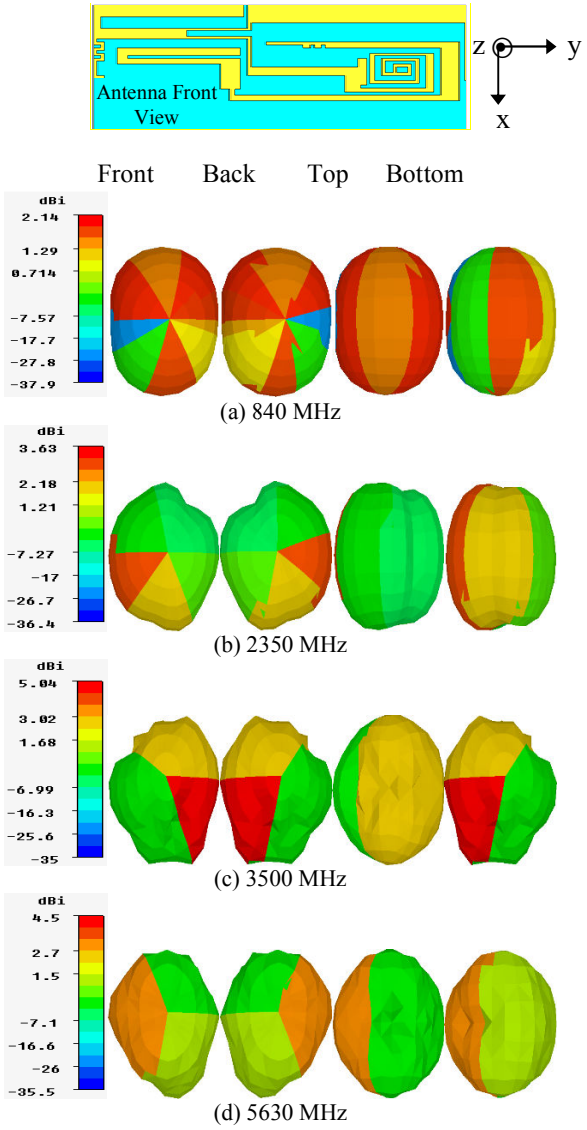

Fig. 14 Simulated three-dimensional (3D) total power radiation patterns of the proposed antenna's front, back, top and bottom views at: (a) 840, (b) 2350, (c) 3500 and (d) 5630MHz

SAR simulations have been carried out using CST Microwave Studio software, where the simulation model is shown in Fig. 15 and the SAM phantom material parameters are given in Table II. The Specific Anthropomorphic Mannequin (SAM) phantom head (PH) shown in Fig. 15 is modeled by a shell filled with a liquid which represents a conservative estimate of the material properties of the human head. The advantage of this model is that measurements can be carried out in reality. The proposed antenna enclosed in the plastic case is placed with a slant angle of 60° and the distance between the SAM phantom head and system ground plane is reasonably chosen to be 6 mm for testing SAR values. The SAR is calculated over 1 gram of the human tissue mass. According to United States regulations, the international SAR limit recommended for mobile phones is 1.6 W/kg taken over a volume of 1 gram of tissue [22]. The antenna is facing in the

opposite direction from the SAM head as depicted in Fig. 15. Results for the central frequencies of the operating bands in the proposed antenna are provided in Table III, and the impedance matching level at the testing frequency is also given. The obtained 1-g SAR values are all meet the limit of 1.6 W/kg with maximum value of 1.251 W/kg at 1800 MHz and the minimum value is 0.841 W/kg at 5630 MHz. The SAR value is the highest at 1800 MHz due to the fact that the whole antenna structure (including feeding strip, coupling strip and the ground plane) is radiating effectively, compared to other frequencies, at this frequency as shown in Fig. 15. At 5630 MHz we have the lowest SAR value and this can be explained by refereeing to Fig. 11 (f), where the ground plane effect is almost negligible and the only part of the antenna radiating is the feeding strip.

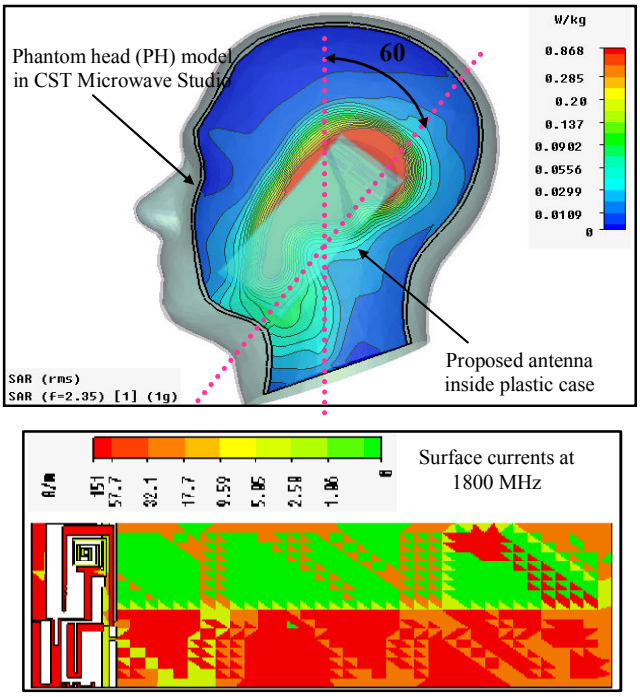

Fig. 15 SAR simulation model using SAM phantom head provided by CST and Surface currents distribution at 1800 MHz.

TABLE II
SAM PHANTOM MATERIAL PARAMETERS

SAM phantom material	Relative permittivity(ε_r)	Conductivity (S/m)	Density (Kg/m^3)
SAM Liquid	42	0.99	1000
SAM Shell	5	0.0125173	0

TABLE III
THE SIMULATED 1-GSAR VALUES FOR THE PROPOSED ANTENNA AND THE RETURN LOSS GIVEN IS THE IMPEDANCE MATCHING LEVEL AT TESTING FREQUENCY FOR BOTH CASES, WITH AND WITHOUT THE PHANTOM HEAD

Frequency (MHz)	730	920	1800	2350	3500	5630
1-g SAR (W/Kg)	0.732	0.924	1.251	0.871	0.634	0.184
Return loss (dB) With PH	7.4	11.4	10.5	13.5	8.4	8.2
Return loss (dB) Without PH	11.7	7.3	8.9	18.7	9.97	6.64

V. CONCLUSION

In this work, a multiband coupled-fed planar printed monopole antenna able to operate efficiently in multiple communication standards by modifying the system ground plane has been proposed. After studying the coupled-fed structure functionality and the effect of the slotted ground plane, it has been concluded that this combination in a mobile phone antenna help to achieve good matching and radiation characteristics in the regions of interest. In the low frequency region, which is usually a big challenge for engineers, the bandwidth improvement and resonant tuning have been an easy task by the presented technique. Significant improvement is obtained in the high frequency regions as well. Thus, the presented technique can be an alternative approach in those platform where is sufficient flexibility to make modifications in the ground plane exists. Four operating modes at return loss better than 6 dB have been generated to cover LTE 700/2300/2500, GSM 850/900/1800/1900, UMTS, WiMAX 3500, WLAN 2400/5200/5800. The main design parameters of the proposed antenna are studied and discussed. A comparison between two simulation software (CST and HFSS) has been applied to verify antenna performance. The simulated characteristics including return loss, antenna gain, radiation patterns, radiation efficiency and SAR are provided to validate the proposed antenna. The antenna exhibits a great potential for multiband mobile communication applications.

REFERENCES

[1] GZhinong Ying, "Antennas in Cellular Phones for Mobile Communications", *Proceedings of the IEEE,* Vol. 100, No. 7, July 2012.
[2] K. L. Wong, "Planar antenna for wireless communications", *Willy*, New York, 2003.
[3] Jin-Hua Chen, Young-Ling Ban and Li-Jun Ying, " Compact PIFA using capacitive coupled-fed for LTE/GSM/UMTS WWAN operation in mobile application", *Cross Quad-Regional Radio Science and Wireless Technology Conference*, 2011
[4] K. L. Wong, and T. W. Kang, "GSM850/900/1800/1900/UMTS printed monopole antenna for mobile phone application", *Microwave Opt. Technol. Lett*., Vol. 50, pp.3192-3198, 2008.
[5] A. Ismahayati, P.J Soh and F. Malek, "Design and Simulation of a Sierpinski Carpet FractalPIFA for WLAN and HiperLAN Application", *Proceedings of IEEE Asia-Pacific Conference on Applied Electromagnetics (APACE)*, 2010
[6] M. S. Sharawi, M. A. Jan and D. N. Aloi, "Four-shaped 2 × 2 multi-standard compact multiple-input-multiple-output antenna system for long-term evolution mobile handsets", *IET Microw. Antennas Propag,* Vol. 6, pp. 685-696, 2012.
[7] Byoung-Nam Kim, Seong-Ook Park, Jung-Keun Oh and Gwan-Young Koo, "Wideband built-In antenna with new crossed C-shaped coupling feed for future mobile phone application", *IEEE Antennas and Wireless Propag Letters,* Vol. 9, 2010.
[8] D. G. Kang and Y. Sung, "Coupled-fed planar printed shorted monopole antenna for LTE/WWAN mobile handset applications", *IEEE Microw. Antennas and Propag,* Vol. 6, pp1007-1016, 2012.
[9] Li-Jun Ying, Young-Ling Ban and Jin-Hua Chen, "Low-profile coupled-fed printed PIFA for internal seven-band LTE/GSM/UMTS mobile phone antenna", *Cross Quad-Regional Radio Science and Wireless Technology Conference*, July. 2011.
[10] Chan-Woo Yang, Young-Bae Jung and Chang Won Jung, "Octaband internal antenna for 4G mobile handset", *IEEE Antennas and Wireless Propag Letters,* Vol. 10, 2011.
[11] Fang-Hsien Chu and Kin-Lu Wong, "Planar printed strip monopole with a closely-coupled parasitic shorted strip for eight-band LTE/GSM/UMTS mobile phone", *IEEE transaction on antennas and propag,* Vol. 58, No. 10, October. 2010.

[12] Shu-Chuan Chen and K. L. Wong, "Small-Size 11-Band LTE/WWAN/WLAN internal mobile phone antenna", *Microwave Opt. Technol. Lett*., Vol. 52, No. 11, November 2010.
[13] C. J. Wang and J. W. Wu, "CPW-fed two-arm spiral slot antenna", *in Proc. Int. Conf. TENCON*, pp. 1-4, 2007.
[14] Y. W. Chi and K. L. Wong, "Compact multiband folded loop chip antenna for small-size mobile phone", *IEEE transaction on antennas and propag,* Vol. 56, No. 12, pp. 3797-3803, December. 2008.
[15] Li. Wei-Yu, "Internal LTE/WWAN handset antenna integrated with solar cells for performance improvement", *Antennas and Propag Society International Symposium (APSURSI),* 2012 *IEEE.*
[16] M. A. C. Niamien, Laurent Dussopt and Christophe Delaveaud, "A compact dual-band notch antenna for wireless multistandard terminals", *IEEE Antennas and Wireless Propag Letters,* Vol. 11, 2012.
[17] R. Hossa, A. Byndas and M. Bialkowski, "Improvement of compact terminal antenna performance by incorporating open-end slots in ground plane," *IEEE Microwave and Wireless Components Letters*, vol. 14, No. 6, June 2004.
[18] C. T. Lee and K. L. Wong, "Planar monopole with a coupling feed and an inductiveshorting strip for LTE/GSM/UMTS operation in mobile phone", *IEEE Antennas and Wireless Propag Letters,* Vol. 58, No. 7, July 2010.
[19] J. H. Jung and I. Park, "Electromagnetically coupled small broadband monopole antenna", *IEEE Antennas and Wireless Propag Letters,* Vol. 2, pp. 349-351, 2003.
[20] M. Kozlov and R. Turner, "A comparison of Ansoft HFSS and CST microwave studio simulation software for multi-channel coil design and SAR estimation at 7T MRI", *PIERS ONLINE*, Vol. 6, No. 4, 2010.
[21] S. I. Al-Mously and M. M. Abousetta, "A novel cellular handset design for an enhanced antenna performance and a reduced SAR in the human head," *International Journal of Antennas and Propag,* March 2008, Article ID 642572.
[22] S. Khalatbari, S. Dariush, A. A. Mirzaee and H. A. Sadafi, "Calculating SAR in two models of the human head exposed to mobile phones radiation at 900 and 1800 MHz", *Progress in EM research Syp, PIER online,* Vol. 2, pp. 104-109, 2006.